CSIRO PUBLISHING

Australian Journal of Physics

Volume 52, 1999

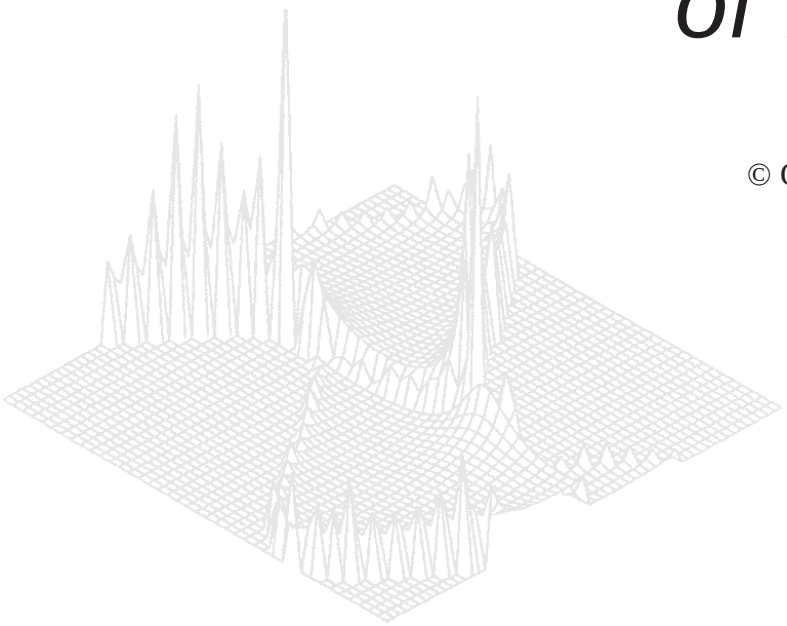

A journal for the publication of
original research in all branches of physics

www.publish.csiro.au/journals/ajp

All enquiries and manuscripts should be directed to
Australian Journal of Physics
CSIRO PUBLISHING
PO Box 1139 (150 Oxford St)
Collingwood Telephone: 61 3 9662 7626
Vic. 3066 Facsimile: 61 3 9662 7611
Australia Email: peter.robertson@publish.csiro.au

Published by **CSIRO** PUBLISHING
for CSIRO Australia and
the Australian Academy of Science

Aust. J. Phys., 1999, **52**, 523–35

Cold Target Helium Recoil Ion Momentum Imaging: Understanding Correlated Electron Motion in the Double Ionisation Process*

H. Schmidt-Böcking,[A] *V. Mergel,*[A] *R. Dörner,*[A] *H. Bräuning,*[A,B,C] *M. Achler,*[A] *L. Spielberger,*[A] *O. Jagutzki,*[A] *T. Weber,*[A] *Kh. Khayyat,*[A] *J. Ullrich,*[D] *C. L. Cocke,*[B] *M. H. Prior,*[C] *Y. Azuma,*[E] *Y. Awaya*[F] *and T. Kambara*[F]

[A]Institut für Kernphysik, Universität Frankfurt,
August Euler Str. 6,
D-60486 Frankfurt, Germany.
[B]Department of Physics, Kansas State University,
Manhattan, KS 66506, USA.
[C]LBNL, Berkeley, CA 94720, USA.
[D]Fakultät für Physik, Universität Freiburg, Germany.
[E]Photon Factory, Tsukuba, Japan.
[F]RIKEN, Wako-shi, Japan.

Abstract

Novel imaging techniques enable a highly efficient detection of ions and electrons from ionising multi-fragmentation processes of atoms and molecules induced by photons and charged particles. From position and time-of-flight measurements the vector momenta of these fragments are determined. These devices combine 4π solid angle with high resolution in momentum space. They deliver multi-dimensional images of the multi-particle break-up processes. These fully differential cross sections unveil the physical processes dominating the reaction. We discuss double ionisation of He induced by photons and fast protons, which is one of the most fundamental two-electron systems. New results are presented. In a speculative manner the future perspectives with respect to the investigation of dynamical electron– electron correlation are discussed.

1. Introduction

The investigation of few-particle transitions in atoms or molecules induced by photons or charged particles is a fascinating testground for our understanding of many-body dynamics in quantum mechanics. Dynamics is the real basis of subatomic nature. The picture of stationary structures only exists in the fictitious world of theory. The dynamics of many-body Coulomb systems contains therefore all the secrets of our every-day world. In quantum mechanical theory (so far mostly stationary approximations) atomic and molecular many-particle reactions are characterised by fully differential cross sections (FDCS), i.e. cross sections differential in all observables of the final state. In an ionisation process these observables are typically the vector momenta, spins and possible internal excitations of the fragmenting reaction products. According to our quantum mechanical knowledge such FDCS provide the most stringent test for theory. Any

* Refereed paper based on a contribution to the Australia–Germany Workshop on Electron Correlations held in Fremantle, Western Australia, on 1–6 October 1998.

 10.1071/PH99020 0004-9506/99/030523$05.00

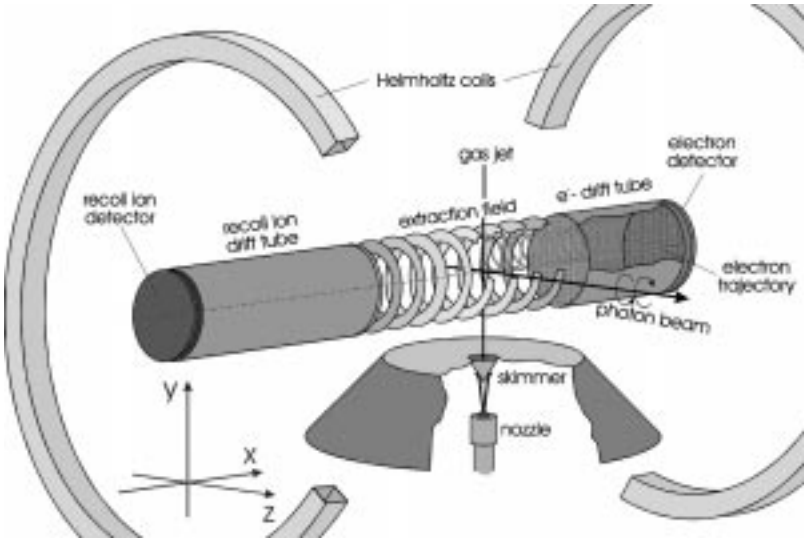

Fig. 1. A typical COLTRIMS setup. The gas nozzle and thus the gas before entering the supersonic expansion area is cooled to 15–30 K. After passing the skimmer the supersonic gas jet has a diameter of $1 \cdot 1$ mm at the intersection with the photon or charged particle beam. The electron detector is located on one side of the spectrometer (here the right side) and the ion detector on the opposite side. A set of Helmholtz coils provides a homogeneous field for guiding the electrons towards the electron detector. [From Achler (1998).]

integration over observables often masks important characteristics of the process. In turn, experimental FDCS directly unveil mechanisms of the many-particle transition. Tremendous progress in measuring such FDCS has been made in the field of (e, 2e) collisions (see Coplan *et al.* 1994; McCarthy and Weigold 1991; Lahmam-Bennani 1991 for reviews) and (γ, 2e) experiments by detecting two electrons in coincidence (see e.g. Schwarzkopf *et al.* 1993, 1994; Schwarzkopf and Schmidt 1995; Huetz *et al.* 1994; Dawber *et al.* 1995; Lablanquie *et al.* 1995; Viefhaus *et al.* 1996*a*, 1996*b*; Wightman *et al.* 1998). The newly developed multi-fragment imaging microscope for atomic collisions and its application is the subject of this paper.

Cold target recoil ion momentum spectroscopy (COLTRIMS) is the key technology for such kinematically complete experiments with 4π solid angle (see Fig. 1). For reactions with only two particles in the final state, such as photo single ionisation, the recoil-ion measurement already delivers complete momentum information. For photo single ionisation the recoil-ion measurement is equivalent to the detection of the photo-electron. For more complex reactions with n particles in the final state, $(n-1)$ of those particles have to be detected to yield complete information on the n particle momentum balance. Also, in principle, the experimentalist is free to choose which of the particles to detect, and it is advantageous to detect the recoil ion. One reason is that with the help of a weak electric field all recoils ions can be projected onto one position-sensitive detector and thus the recoil-ion time-of-flight can be measured with very high precision. Furthermore, the recoil-ion momentum itself, even if one integrates over all other observables, is already a rich source of information, in particular

because the ion time-of-flight measurement yields additional information on the charge state and thus the multiplicity of the fragmentation process.

COLTRIMS thus provides very high multi-fragment imaging efficiency (some 10%) and simultanously high momentum resolution. As we show below, even differential cross sections in the regime of microbarns can be measured under gas target single collision conditions. With traditional techniques such measurements would have taken hundreds of years. Therefore, we believe that by using this new method we can explore in an unprecedented manner the multi-particle dynamics in atomic and molecular physics.

2. Experimental Technique

The basic principle of high resolution 4π imaging spectrometers is identical for ion and electron detection. They are based on a small reaction volume (typically below 1 mm^3) from which the fragments are guided by electric and magnetic fields to large area position-sensitive detectors. The momenta of the electron and ion can then be calculated from their time-of-flight and the position where these particles hit the detectors. The ion momenta resulting from atomic reactions are typically in the range of a few atomic units (a.u.) and their energies in the μeV–meV regime. This is comparable or even smaller than the thermal motion of the atoms at room temperature ($4 \cdot 6$ a.u. for He). Thus, one has to prepare an internally cold atomic target for the collision. This is presently achieved by using supersonic gas-jet targets. A further improvement in resolution is envisaged by the future use of laser-cooled targets (Wolf and Helm 1997). In all high resolution measurements using COLTRIMS supersonic gas-jet targets have been used. The gas jet is formed by expanding the gas through a 30 μm hole. In some cases the nozzle and the gas are precooled to 15–30 K using a cryogenic cold head to further improve the resolution. From this expansion a supersonic jet is formed and the He atoms have a mean speed proportional to the square root of the nozzle temperature. The momentum distribution around the mean value is given by the speed ratio of the expansion (Brusdeylins *et al.* 1989). The precooling helps to achieve a narrow momentum distribution even when small turbo pumps are used. About 1 cm above the nozzle the inner part of the preformed gas jet enters the scattering chamber through a skimmer of $0 \cdot 3$ mm diameter. A typical operating condition for precooled one stage jets with small turbo pumps (260 litre/s) is a driving pressure of 400 mbar. Under these conditions the typical pressures are 5×10^{-4} mbar in the source chamber and a few 10^{-5} mbar in the target region, 3 cm above the skimmer. The gas jet leaves the scattering chamber into a separately pumped jet dump. In other experiments two-stage jets (Jardin *et al.* 1993; Moshammer *et al.* 1996*b*) or jets backed with 8000 litre/s diffusion pumps (Jagutzki *et al.* 1996; Spielberger *et al.* 1995) are successfully used.

The ions are created in the overlap volume of the gas jet with the projectile beam. Different designs for recoil-ion and electron spectrometers have been used. In a first version a homogeneous electric field followed by a drift tube guided the ions to a position-sensitive channel plate (Jagutzki 1994; Mergel 1994; Mergel *et al.* 1995*a*, 1995*b*; Dörner *et al.* 1994, 1995*b*). With this homogeneous field spectrometer Mergel and coworkers reported a resolution of $0 \cdot 26$ a.u. (Mergel *et al.* 1995*a*). A very flexible combination of electric fields for ion detection and

magnetic fields for guiding the electrons has been used at GSI (Moshammer *et al.* 1994, 1996*a*, 1997*a*, 1997*b*; Unverzagt *et al.* 1996). This 'momentum microscope' is discussed in detail in Moshammer *et al.* (1996*b*). In all spectrometers with homogeneous fields the ion-momentum resolution is restricted by the extension of the overlap volume. To circumvent this restriction Mergel (1996) has designed a field geometry which focuses in three dimensions. An electrostatic lens in the extraction region focuses different starting positions perpendicular to the extraction field onto one point on the detector. In the third direction different starting points along the field lead to the same time-of-flight. Thus, a high resolution can be achieved even with a gas target extended over several mm. With this spectrometer a resolution of $0 \cdot 07$ a.u FWHM, which is close to the internal temperature of the gas jet, has been reached (Dörner *et al.* 1995*a*). Details on the field geometry can be found in Dörner *et al.* (1998*a*) and Mergel (1996). A typical COLTRIMS setup is shown in Fig. 1.

Due to the low energy of the recoiling ions a moderate field of a few V/cm is sufficient to collect all ions onto the detector. The same field is used to guide the electrons in the opposite direction. If one chooses a distance of 2 cm from the target region to the electron detector a 4π collection efficiency can be reached only for very low energy electrons (1–5 eV). In fast particle collisions, however, often electrons with higher energies are created. To guide such electrons to the detector, Moshammer and coworkers have superimposed on the electric field a homogeneous magnetic field yielding 4π detection efficiency up to 30 eV electron energy (Moshammer *et al.* 1996*b*). Electrons with higher energies can be accessed by increasing the magnetic and electric fields. Such electron imaging spectrometers with magnetic confinement are used with great success in ion impact (Moshammer *et al.* 1995, 1996*a*, 1996*b*, 1997*a*, 1997*b*) and in photo-ionisation studies (Bräuning *et al.* 1997, 1998; Dörner *et al.* 1998*b*).

3. Experimental Results

(3a) Photon Induced Double Ionisation of Helium

A particularly interesting case of an atomic few-body reaction is double ionisation of He by a single photon. This process is an interesting probe of the effects of dynamic electron correlation, one of the hottest topics in today's atomic collision physics. Since the photon momentum is negligibly small compared with the momenta of all particles involved in the reaction process, it does not therefore perturbate the initial momentum structure of the entangled helium system. Thus double ionisation by one photon 'projects' the internal momentum structure into the final continuum. To what extent this initial momentum structure is present in the final momenta depends on the importance of the so-called final state three-body Coulomb interaction. In the case where we know the angular momentum of the incoming photon (e.g. by using circularly polarised light), we probe left/right handedness of the internal electronic motion of the system.

To illuminate how one photon can couple to two electrons, it is instructive to compare the final-state momentum distributions of the He^{2+} ions and the electrons created by photoabsorbtion. Fig. 2*b* shows the momentum distribution of the ions for double ionisation. Since the two electrons in the continuum can share the excess photon energy and emerge with various relative angles, the ion

momenta are no longer restricted to the surface of spheres in momentum space. The maximum ion momentum at a given photon energy is

$$k_{\text{ion}} = 2\sqrt{(E_\gamma - E_{\text{bind}})}\,, \tag{1}$$

where E_{bind} is the sum of the ionisation potentials for both electrons. This momentum, which is indicated by the outer circle, corresponds to the situation where both electrons escape with equal energy in the same direction. As already shown by Schwarzkopf *et al.* (1993) this is inhibited by the electron electron repulsion, and thus the cross section falls to zero towards the circular line. The cross section has also a node at ion momentum zero. This corresponds to the case where both electrons emerge with equal energy in opposite directions. As has been shown by several authors, this is prohibited by a selection rule (Schwarzkopf *et al.* 1993; Maulbetsch and Briggs 1993; Malegat *et al.* 1997).

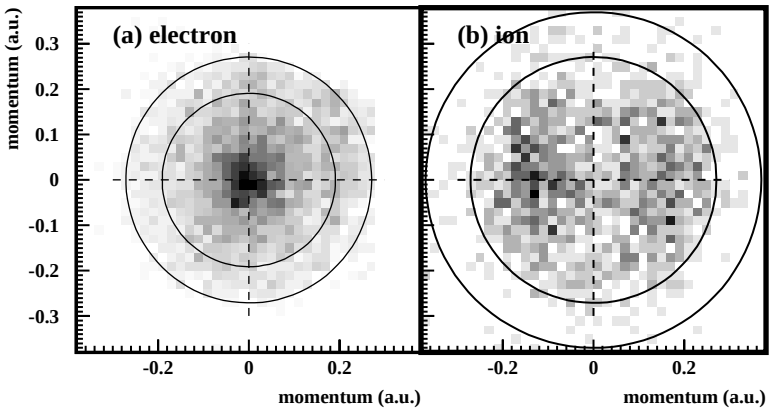

Fig. 2. Density plots of projections of the momentum distribution from double ionisation of He by 80·1 eV linearly polarised photons. The x and y components of the momentum are plotted on the horizontal and vertical axes respectively. The polarisation vector of the photon is in the x direction and the photon propagates in the z direction. Only events with $-0{\cdot}1 < k_{rz} < 0{\cdot}1$ a.u. are projected onto the plane. (*a*) Distribution of single electron momenta ($\mathbf{k}_1$ or $\mathbf{k}_2$). The outer circle locates the momentum of an electron which carries the full excess energy. (*b*) Recoil (or $-\mathbf{k}_r$) momentum distribution. The outer circle indicates the maximum calculated recoil momentum and the inner circle is the locus of events for which the $\mathbf{k}_r$ motion has half the excess energy. [From Dörner *et al.* (1996).]

For comparison with the ionic momentum distributions we display this known electronic distribution in cartesian momentum coordinates for 1 eV excess energy in Fig. 2*a*. The striking difference between the electronic and ionic distributions invites speculation on the mechanisms of photo double ionisation. The photon acts upon a charge dipole in the atom. This dipole can be thought of as consisting of the positive ion on one pole and either the centre of charge of the electron pair or one of the electrons on the other pole. In either case the first step of the absorption of the photon will imprint the dipolar characteristics of the linearly polarised photon on the distribution of the fragments of a charge dipole. The experiment

indicates that the momentum distribution of the nucleus shows a memory of this absorbtion of the photon, while it is completely smeared out in the electron momentum distribution. If one favours the electron pair as the ion's counterpart in the photon-absorbing charge dipole, the subsequent breakup motion of the electron pair is mainly responsible for the electron distribution. The direction of this breakup given by the electron-pair relative momentum $\mathbf{k}_{\mathrm{R}} = \frac{1}{2}(\mathbf{k}_1 - \mathbf{k}_2)$ has been found for 1 eV excess energy to be mainly perpendicular to the photon polarisation axis. For additional discussion see Dörner *et al.* (1996) and Feagin (1996). The picture of such a collective motion of the electron pair is most plausible close to threshold. At higher photon energy it seems more appropriate to think of a (single-electron + ion dipole) absorbing the photon. Of course, then electron correlation is indispensable to double ionisation. One concludes that it is this electron–electron interaction which smears out the observed recoil-ion dipole pattern . This point of view is in qualitative agreement with the model of Samson (1990) and Samson *et al.* (1992) which views photo double ionisation as photo-absorbtion by one electron followed by internal electron impact ionisation.

An overview of the three-body continuum in the momenta of the two electrons is given in Fig. 3. It shows the momentum of one electron with respect to the other at 1 and 20 eV above the double ionisation threshold. All three particles are necessarily in one plane (following from momentum conservation). This internal plane of the breakup has some orientation to the electric field vector ϵ of the linearly polarised photon beam.

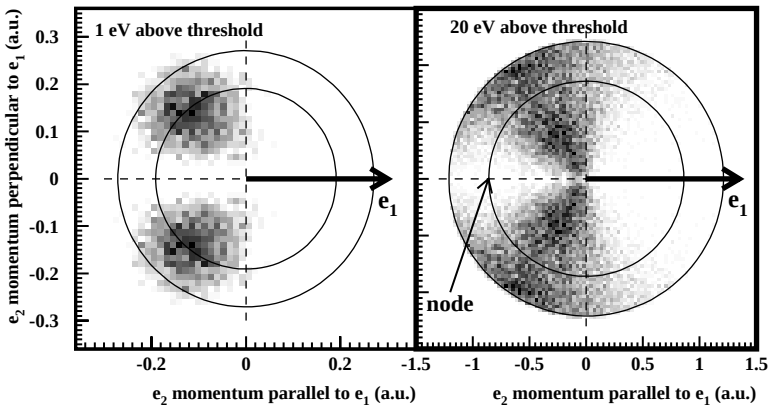

Fig. 3. Photo double ionisation of He at 1 and 20 eV above threshold by linearly polarised light. Shown is the momentum distribution of electron 2 for fixed direction of electron 1 as indicated. The plane of the figure is the internal momentum plane of the three particles. The data are integrated over all orientations of the polarisation axis with respect to this plane. The figure thus samples the full cross sections, and all angular and energy distributions of the fragments. The outer circle corresponds to the maximum possible electron momentum and the inner one to the case of equal energy sharing (see text for details).

In Fig. 3 we show the momenta of the electrons in this internal plane integrated over all directions of ϵ. Electron 1 is chosen along the positive x-axis of the figure (shown by the arrow). The full cross section, all energy sharings and all angles,

are sampled in this figure. Each circle on this plane corresponds to a particular energy sharing. The outer circle gives the maximum available momentum (i.e. extremely unequal energy sharing), while the inner circle corresponds to equal energy sharing. As has been shown already by the work using coincident electron detection (see e.g. Schwarzkopf *et al.* 1993, 1994; Schwarzkopf and Schmidt 1995; Huetz *et al.* 1994), two main features determine the momentum distribution: the effect of electron repulsion and a selection rule from the $^1P^0$ symmetry of the final state. Electron repulsion at these low excess energies leads to an emission of the electrons to opposite half spheres. There are almost no events on the right half of the figure corresponding to two electrons going to the same internal half plane. As can be expected from the velocity of the particles, this backward emission effect is slightly more pronounced at 1 eV than at 20 eV. Second, for a $^1P^0$ two body state $\mathbf{k}_1 = -bfk_2$, i.e. back to back emission of equal energy electrons, is prohibited (see selection rule C in Maulbetsch and Briggs 1995). For 1 eV the data show that this node extends all the way along the x-axis. Thus at such low energies back-to-back emission is suppressed at all energy sharings, but even so this is not a strict selection rule (see also Lablanquie *et al.* 1995). At 20 eV the node is really centred at $\mathbf{k}_1 = -bfk_2$ (indicated by the arrow). This presentation shows strikingly that this node is internal to the three-body system and has nothing to do with ϵ, since the data are integrated over all orientations of ϵ.

An interesting twist is added to this three-body breakup if one introduces a chirality in the initial state by inducing the transition with circular instead of linearly polarised light. The question arises how, or if at all, the chirality of the photon is transferred to the three-body continuum. It was first pointed out by Berakdar and Klar (1992) that such an effect, termed dichroism, might exist even for He double ionisation. Viefhaus and coworkers (Viefhaus *et al.* 1996*b*) found the first experimental evidence for this effect. The two electrons and the photon axis can span a tripod which could have a handedness if its two legs defined by the electron momenta are distinguishable, i.e. the electrons have unequal energy. This shows up strongest if the three-body plane (as shown in Fig. 3) is held fixed perpendicular to the photon axis. At 20 eV above threshold, Fig. 4 shows the momentum distribution of the ion and electron 2 in this plane. The momentum of electron 1, which is chosen to be the faster one, is fixed along the x-axis. Comparison with Fig. 3 as well as between left and right circularly polarised light shows that dichroism is a huge effect in this system. While for linearly polarised light the upper and lower half of Fig. 4 are necessarily symmetric, this symmetry is broken for circularly polarised light. A detailed comparison of these experimental results with 3C calculations can be found in Mergel *et al.* (1998). In general the agreement between 3C theory and experiment is much worse for circularly polarised light (Mergel *et al.* 1998) than for linearly polarised light.

A detailed discussion of the possible reasons for the disagreement between theory and experiment for circularly polarised photons is given by Kheifets and Bray (1998). Their conclusion is that the experimental results for circularly polarised light cannot be within the quoted range of errors. After a very careful search for any possible as yet undiscovered source of experimental error we believe that our data are correct. But nevertheless, because the observed disagreement would have quite fundamental consequences, we have recently repeated these

measurements with improved photon beam bunching. However, a careful data analysis is quite time consuming and it will take a few months to make any final conclusion.

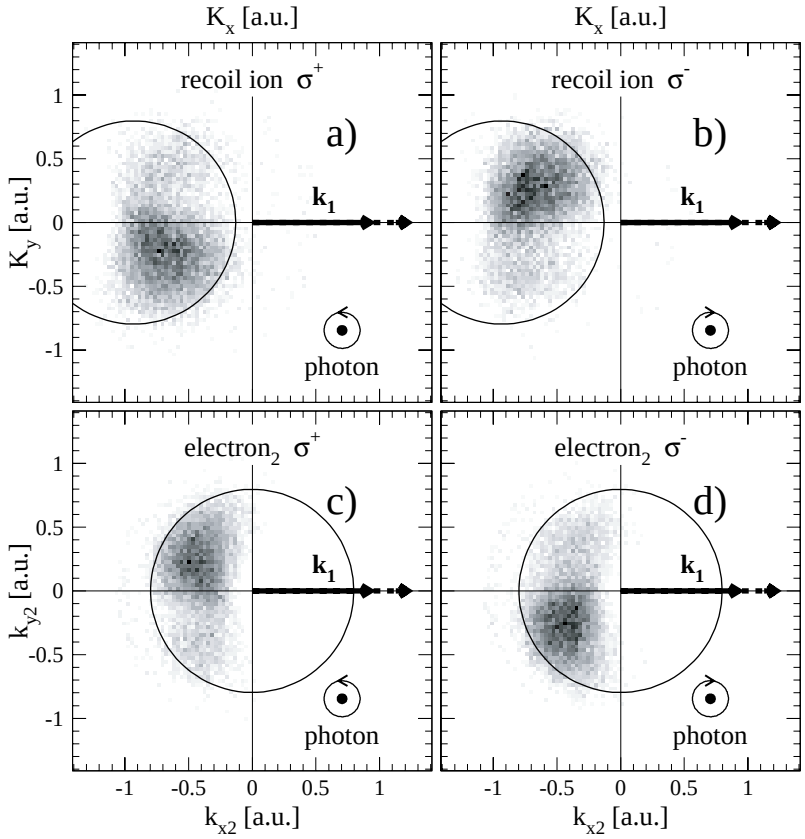

Fig. 4. Recoil ion and electron momentum distribution in the x–y plane both for σ^+ and σ^- as indicated. We fixed e_1 within $0{\cdot}9 < k_{x1} < 1{\cdot}2$ a.u. and with $k_{y1} = k_{z1} = 0$. The wave vector $\mathbf{k}_\gamma$ points out of the plane of the page. Circles show the maximum magnitude of $\mathbf{K}$ and $\mathbf{k}_2$. The grey scale represents the fivefold differential cross section on a linear scale. [From Mergel *et al.* (1998).]

(3b) Transfer Ionisation of Helium by Fast Protons

Another interesting way to probe electron–electron correlations in the helium ground state is billard playing with bound electrons under strongly controlled kinematic conditions. We have chosen the transfer ionisation reaction with a proton as knocking ball (projectile), where one of the target electrons is emitted in the continuum and the other is captured by the proton. Using the COLTRIMS technique two interesting reaction channels can be clearly separated in momentum space. First, the so-called e–e–Thomas process (see Fig. 5) and, second, the so-called kinematic capture plus independent ionisation. Details of the kinematic equations are described in the dissertation by Mergel (1996). Measuring the complete momentum balance for the three-particle final state (H^0,

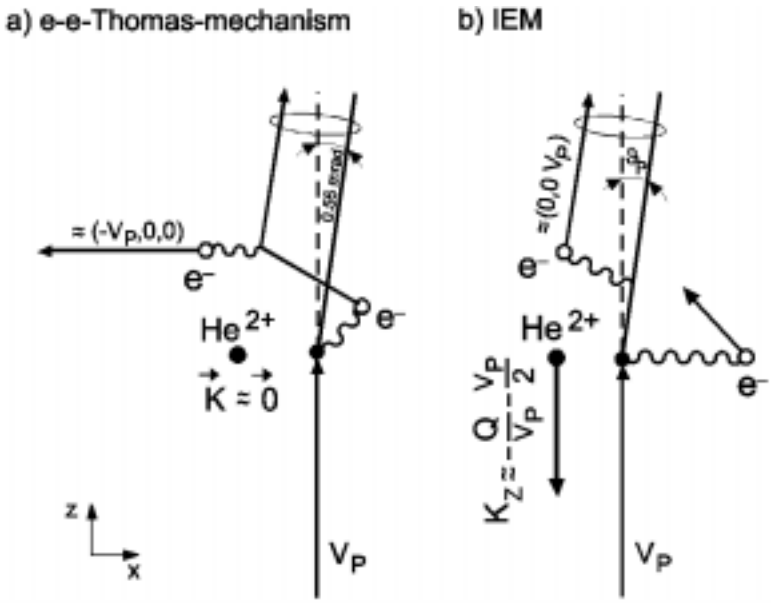

Fig. 5. Kinematics of (a) the correlated e–e–Thomas process and (b) the two-step process of kinematic capture and ionisation through independent projectile electron interactions.

He^{2+}, e) the different reaction channels (i.e. different billard collisions) can be kinematically separated and its differential cross sections as well as the correlated three particle, in particular the electron–electron kinematics, can be determined experimentally. In Fig. 6 the recoil-ion momentum distribution (for 1 MeV proton impact and for a H^0-scattering angle of $0{\cdot}55$ mrad) the recoil-ion momentum distribution is shown in a contour plot. Two peaks are observed, where one near $(K_x, K_z) = (0, 0)$ corresponds to the e–e–Thomas process, while the other at $(K_x, K_z) = (-1{\cdot}8, -2{\cdot}8)$ (in atomic units) is due to the kinematic capture plus independent ionisation process. As discussed by Mergel *et al.* (1997) the total e-e–Thomas cross section follows a $v_P^{-7\cdot4\pm1\cdot0}$ power law, which is in contradiction to the proton velocity dependence of v_P^{-11}, predicted by the classical calculation of Thomas and the second Born approximation (see Mergel 1996). Furthermore, the position of the kinematic plus independent ionisation peak is in clear contradiction to independent particle scattering laws. The reasons for both discrepancies are still unclear. The momentum vector of the emitted second electron always points in the direction of the He^{2+} recoil-ion momentum vector (transverse). This cannot be explained by post-collision effects, since the recoil ion is about 10,000 times slower than the emitted electron. We believe that this kinematic capture plus independent ionisation channel is a very sensitive probe for extremely selective electron–electron motion, i.e. a dynamical e–e correlation. These data are discussed in detail in Mergel (1996).

4. Outlook

Momentum-space imaging provides new and spectacular views of many-body breakup processes of Coulombic systems. It combines high resolution in momentum

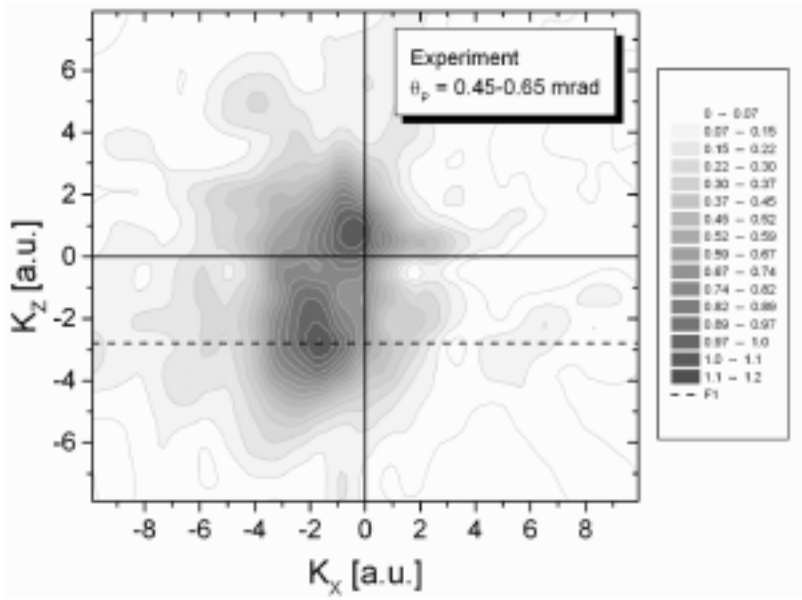

Fig. 6. Recoil-ion distribution showing a contour plot of the TDCS $d^3\sigma/d\theta_P dK_x dK_z$ as a function of K_x and K_z at $E_P = 1$ MeV and a scattering angle of $\theta_P = 0{\cdot}55 \pm 0{\cdot}1$ mrad (which points to the right). The dashed line shows the calculated position of the kinematic capture plus independent ionisation and the left vertical line shows the momentum transfer to the whole target corresponding to the scattering angle range of $\theta_P = 0{\cdot}55 \pm 0{\cdot}1$ mrad.

space (typically $<0{\cdot}1$ a.u.) with 4π solid angle for all fragments. In many cases such kinematically complete images directly 'display' the processes responsible for the many-body Coulomb interaction. Thus, some long-standing puzzles in atomic collision physics have recently been investigated by using this approach. However, many new questions and challenges to theory were raised, as shown for the few data examples presented above.

Since this paper originated as a contribution to a workshop the invited speaker (HSB) would like to raise some questions which are not authorised by the other co-authors. Looking in detail into the kinematics of the transfer ionisation data of p on He collisions, these differential data show surprising structures in the correlated motion pattern of the two electrons (kinematical capture) which are hard to explain in the independent electron picture. As mentioned above (when H^0 is scattered under approximately $0{\cdot}5$ mrad), the momentum vector of the 'second' emitted electron coincides always with the direction of the recoil-ion momentum vector and never points to the opposite side or out of the nuclear scattering plane. This observation could be taken as a sign that the two ground state electrons in the moment of capture (duration some 10 attosec) have a unique relation in their motion (when one is captured) or that (for so far unthinkable reasons) the three-body reaction itself produces such an asymmetry, i.e. that a three-body scattering process with an entangled system acts in a helical way [nobody could ever test whether three-body Coulomb scattering of entangled particles breaks the well-known two-particle Coulomb symmetries (parity, time, etc.)]. Nevertheless,

either in the case where the initial relative motion of two electrons shows this correlation or in the case where the three-body Coulomb scattering of entangled particles is responsible for this asymmetric momentum structure, this observation could be very fundamental and needs further investigation. Since these data might be of fundamental interest one of us (VM) is repeating and extending these measurements with an advanced COLTRIMS system to ensure that no unknown source of error creates the observed asymmetric structures in the electron emission pattern.

Acknowledgments

The work was financially supported by DFG, BMFT and by the Division of Chemical Sciences, Basic Energy Sciences, Office of Energy Research, US Department of Energy. One of us (RD) was supported by the Habilitanden Programm der DFG. HB and RD acknowledge support from the Alexander von Humboldt Foundation. KhK gratefully acknowledges support by the DAAD. VM acknowledges the Studienstiftung des Deutschen Volkes and the DAAD. We also acknowledge financial support from Max Planck Forschungspreis of the Humboldt Foundation. We further acknowledge helpful discussion with our colleagues Y. D. Wang, S. Keller, R. Dreizler, C. Whelan, J. Walters, H. Khemliche, J. Feagin, N. Berrah, J. Briggs, J. Berakdar and R. E. Olson.

References

Achler, M. (1998). PhD thesis, Universität Frankfurt, unpublished.

Berakdar, J., and Klar, H. (1992). *Phys. Rev. Lett.* **69**, 1175.

Bräuning, H. P., Dörner, R., Cocke, C. L., Prior, M. H., Krässig, B., Bräuning-Demian, A., Carnes, K., Dreuil, S., Mergel, V., Richard, P., Ullrich, J., and Schmidt-Böcking, H. (1997). *J. Phys.* B **30**, L649.

Bräuning, H. P., Dörner, R., Cocke, C. L., Prior, M. H., Krässig, B., Kheifets, A. S., Bray, I., Bräuning-Demian, A., Carnes, K., Dreuil, S., Mergel, V., Richard, P., Ullrich, J., and Schmidt-Böcking, H. (1998). *J. Phys.* B **31**, 5149.

Brusdeylins, G., Toennies, J. P., and Vollmer, R. (1989). Twelfth Symp. on Molecular Beams, Perugia, p. 98.

Coplan, M. A., *et al.* (1994). *Rev. Mod. Phys.*, **66**, 985 and references therein.

Dawber, G., Avaldi, L., McConkey, A. G., Rojas, H., MacDonald, M. A., and King, G. C. (1995). *J. Phys.* B **28**, L271.

Dörner, R., Mergel, V., Ali, R., Buck, U., Cocke, C. L., Froschauer, K., Jagutzki, O., Lencinas, S., Meyerhof, W. E., Nüttgens, S., Olson, R. E., Schmidt-Böcking, H., Spielberger, L., Tökesi, K., Ullrich, J., Unverzagt, M., and Wu, W. (1994). *Phys. Rev. Lett.* **72**, 3166.

Dörner, R., Mergel, V., Spielberger, L., Jagutzki, O., Nüttgens, S., Unverzagt, M., Schmidt-Böcking, H., Ullrich, J., Olson, R. E., Tökesi, K., Meyerhof, W. E., Wu, W., and Cocke, C. L. (1995). AIP Conf. Proc. No. 360 (Eds L. J. Dube *et al*)., p. 495 (AIP Press: New York).

Dörner, R., Mergel, V., Zhaoyuan, L., Ullrich, J., Spielberger, L., Olson, R. E., and Schmidt-Böcking, H. (1995). *J. Phys* B **28**, 435.

Dörner, R., Feagin, J., Cocke, C. L., Bräuning, H., Jagutzki, O., Jung, M., Kanter, E. P., Khemliche, H., Kravis, S., Mergel, V., Prior, M. H., Schmidt-Böcking, H., Spielberger, L., Ullrich, J., Unverzagt, M., and Vogt, T. (1996). *Phys. Rev. Lett.* **77**, 1024 [see also erratum in *Phys. Rev. Lett.* **78** (1997) 2031].

Dörner, R., Bräuning, H., Feagin, J. M., Mergel, V., Jagutzki, O., Spielberger, L., Vogt, T., Khemliche, H., Prior, M. H., Ullrich, J., Cocke, C. L., and Schmidt-Böcking, H. (1998). *Phys. Rev.* A **57**, 1074.

Dörner, R., Bräuning, H., Jagutzki, O., Mergel, V., Achler, M., Moshammer, R., Feagin, J., Bräuning-Demian, A., Spielberger, L., McGuire, J. H., Prior, M. H., Berrah, N., Bozek, J., Cocke, C. L., and Schmidt-Böcking, H. (1998). *Phys. Rev. Lett.* **81**, 5776.

Feagin, J. M. (1996). *J. Phys.* B **29**, l551.
Huetz, A., Lablanquie, P., Andric, L., Selles, P., and Mazeau, J. (1994). *J. Phys.* B **27**, L13.
Jagutzki, J. (1994). Dissertation, Unversität Frankfurt, unpublished.
Jagutzki, O., Spielberger, L., Dörner, R., Nüttgens, S., Mergel, V., Schmidt-Böcking, H., Ullrich, J., Olson, R. E., and Buck, U. (1996). *Z. Phys.* D **36**, 5.
Jardin, P., Grandin, J. P., Cassimi, A., Lemoigne, J. P., Gosseling, A., Husson, X., Hennecart, D., and Lepoutre, A. (1993). AIP Conf. Proc. No. 274, p. 291 (AIP Press: New York).
Kheifets, A., and Bray, I. (1998). *Phys. Rev. Lett.* **81**, 4588.
Lablanquie, P., Mazeau, J., Andric, L., Selles, P., and Huetz, A. (1995). *Phys. Rev. Lett.* **74**, 2192.
Lahmam-Bennani, A. (1991). *J. Phys* B **24**, 2401.
McCarthy, I. E., and Weigold, E. (1991). *Rep. Prog. Phys.* **54**, 789.
Malegat, L., Selles, P., and Huetz, A. (1997). *J. Phys.* B **30**, 251.
Maulbetsch, F., and Briggs, J. S. (1993). *J. Phys.* B **26**, 1679.
Maulbetsch, F., and Briggs, J. S. (1995). *J. Phys.* B **28**, 551.
Mergel, V. (1994). Diploma thesis, Universität Frankfurt, unpublished.
Mergel, V. (1996). PhD thesis, Universität Frankfurt (Shaker Verlag: Frankfurt).
Mergel, V., Dörner, R., Ullrich, J., Jagutzki, O., Lencinas, S., Nüttgens, S., Spielberger, L., Unverzagt, M., Cocke, C. L., Olson, R. E., Schulz, M., Buck, U., Zanger, E., Theisinger, W., Isser, M., Geis, S., and Schmidt-Böcking, H. (1995). *Phys. Rev. Lett.* **74**, 2200.
Mergel, V., Dörner, R., Ullrich, J., Jagutzki, O., Lencinas, S., Nüttgens, S., Spielberger, L., Unverzagt, M., Cocke, C. L., Olson, R. E., Schulz, M., Buck, U., and Schmidt-Böcking, H. (1995). *Nucl. Instrum. Methods* B **96**, 593.
Mergel, V., Dörner, R., Achler, M., Khayyat, Kh., Lencinas, S., Euler, J., Jagutzki, O., Nüttgens, S., Unverzagt, M., Spielberger, L., Wu, W., Ali, R., Ullrich, J., Cederquist, H., Salin, A., Olson, R. E., Belkić, Dž., Cocke, C. L., and Schmidt-Böcking, H. (1997). *Phys. Rev. Lett.* **79**, 387.
Mergel, V., Achler, M., Dörner, R., Khayyat, Kh., Kambara, T., Awaya, Y., Zoran, V., Nyström, B., Spielberger, L., McGuire, J. H., Feagin, J., Berakdar, J., Azuma, Y., and Schmidt-Böcking, H. (1998). *Phys. Rev. Lett.* **80**, 5301.
Moshammer, R., Ullrich, J., Unverzagt, M., Schmidt, W., Jardin, P., Olson, R. E., Mann, R., Dörner, R., Mergel, V., Buck, U., and Schmidt-Böcking, H. (1994). *Phys. Rev. Lett.* **73**, 3371.
Moshammer, R., Ullrich, J., Unverzagt, M., Schmitt, W., Jardin, P., Olson, R. E., Mann, R., Dörner, R., Mergel, V., Buck, U., and Schmidt-Böcking, H. (1995). *Nucl. Instrum. Methods* B **107**, 62.
Moshammer, R., Ullrich, J., Kollmus, H., Schmitt, W., Unverzagt, M., Jagutzki, O., Mergel, V., Schmidt-Böcking, H., Mann, R., Woods, C. J., and Olson, R. E. (1996). *Phys. Rev. Lett.* **77**, 1242.
Moshammer, R., Unverzagt, M., Schmitt, W., Ullrich, J., and Schmidt-Böcking, H. (1996). *Nucl. Instrum. Methods* B **108**, 425.
Moshammer, R., Ullrich, J., Kollmus, H., Schmitt, W., Unverzagt, M., Schmidt-Böcking, H., Wood, C. J., and Olson, R. E. (1997). *Phys. Rev.* A **56**, 1351.
Moshammer, R., Ullrich, J., Schmitt, W., Kollmus, H., Cassimi, A., Dörner, R., Dreizler, R., Jagutzki, O., Keller, S., Lüdde, H.-J., Mann, R., Mergel, V., Olson, R. E., Prinz, T., Schmidt-Böcking, H., and Spielberger, L. (1997). *Phys. Rev. Lett* **79**, 3621.
Samson, J. A. R. (1990). *Phys. Rev. Lett.* **65**, 2863.
Samson, J. A. R., Bartlett, R. J., and He, Z. X. (1992). *Phys. Rev.* A **46**, 7277.
Schwarzkopf, O., and Schmidt, V. (1995). *J. Phys.* B **28**, 2847.
Schwarzkopf, O., Krässig, B., Elmiger, J., and Schmidt, V. (1993). *Phys. Rev. Lett.* **70**, 3008.
Schwarzkopf, O., Krässig, B., Schmidt, V., Maulbetsch, F., and Briggs, J. (1994). *J. Phys.* B **27**, L347.
Spielberger, L., Jagutzki, O., Dörner, R., Ullrich, J., Meyer, U., Mergel, V., Unverzagt, M., Damrau, M., Vogt, T., Ali, I., Khayyat, Kh., Bahr, D., Schmidt, H. G., Frahm, R., and Schmidt-Böcking, H. (1995). *Phys. Rev. Lett.* **74**, 4615.
Unverzagt, M., Moshammer, R., Schmitt, W., Olson, R. E., Jardin, P., Mergel, V., Ullrich, J., and Schmidt-Böcking, H. (1996). *Phys. Rev. Lett.* **76**, 1043.

Viefhaus, J., Avaldi, L., Heiser, F., Hentges, R., Gessner, O., Rüdel, A., Wiedenhöft, M., Wielczek, K., and Becker, U. (1996). *J. Phys.* B **29**, L729.
Viefhaus, J., Avaldi, L., Snell, G., Wiedenhöft, M., Hentges, R., Rüdel, A., Schäfer, F., Menke, D., Heinzmann, U., Engelns, A., Berakdar, J., Klar, H., and Becker, U. (1996). *Phys. Rev. Lett.* **77**, 3975.
Wightman, J. P., Cveejanovic, S., and Reddish, T. J. (1998). *J. Phys.* B **31**, 1753.
Wolf, S., and Helm, H. (1997). *Phys. Rev.* A **56**, R4385.

Manuscript received 11 February, accepted 21 April 1999